

Extrusion of small vesicles through nanochannels: A model for experiments and molecular dynamics simulations

Martin Bertrand and Béla Joós*

Département de Physique, Université d'Ottawa, Ottawa, Ontario, Canada K1N 6N5

(Received 12 December 2011; revised manuscript received 10 April 2012; published 18 May 2012)

We propose a model that predicts the final sizes of lipid bilayer vesicles produced by pressure extrusion through nanochannels and we conduct large-scale coarse-grained molecular dynamics simulations of the phenomenon. We show that, to a first approximation independent of pressure, vesicle size can be predicted by a simple geometrical argument that considers an invariable inner vesicle volume enclosed by a finitely extensible lipid bilayer. The pressure dependence is then incorporated in our model by arguing that the effective channel radius decreases with increasing pressure due to a thickening of the lubrication layer between the vesicles and the channel wall. We fit our model to the experimental data of Patty and Frisken [Biophys. J. **85**, 996 (2003)]. We predict that at high pressure, vesicle size significantly depends on channel length and, therefore, flow rate. The CGMD simulations reproduce the physical principles of the model. They also show the build-up of the stress in the vesicle, and typical rupture scenarios as the pressure gradient is increased.

DOI: [10.1103/PhysRevE.85.051910](https://doi.org/10.1103/PhysRevE.85.051910)

PACS number(s): 87.16.D-, 87.10.Tf, 83.50.-v, 82.70.Uv

I. INTRODUCTION

Small unilamellar lipid bilayer vesicles (SUVs), or liposomes, are often synthesized for research and pharmacological applications [1–3]. One of the most popular techniques to produce such soft objects is the pressure extrusion of a vesicle suspension through an array of nanochannels [2,4–7]. Related to this procedure, a long-standing goal has been to be able to predict the average final size of the extruded liposomes given the parameters of the system, which are: lipid nature, concentration of lipids in suspension, temperature, applied pressure, and radius of the nanochannels. Two models have been proposed: the first by Clerc and Thompson [8] refers to the Rayleigh instability [9] and predicts a final vesicle size larger than observed [5–7] and mostly independent of pressure; the second by Patty and Frisken [7] uses the analogy of blowing a bubble through a hole to describe the initial entry of large vesicles in the smaller nanochannels and derives a prediction from an analysis of the system in static equilibrium. Although this second model successfully fits their data, it requires two free parameters that are not clearly linked to the physics of vesicle pressure extrusion and looks at the problem from a static viewpoint. In contrast to this static description our model includes a dynamic (i.e., rheological) description of the extrusion.

Pressure extrusion involves multiple passages through nanochannels, and we can assume that in the final passages, vesicles mostly unilamellar, flow in and out without breaking and their shape goes back and forth between a spheroid outside of the channels and a spherocylinder inside. The spherocylinder has a greater area than the sphere of equal volume. The final vesicles are of a size such that the lipid bilayer can tolerate this area difference. We show that to a first approximation, this prediction is valid. We then incorporate the effects of pressure in our simple geometrical argument using elements of a model of spherocylindrical vesicles flowing in narrow channels developed by Bruinsma [10] to predict

the final sizes of extruded vesicles as pressure is increased. This idea was mentioned by Hunter and Frisken [5] but not exploited. Flow being involved here, it is expected that the length of the channels would be an important parameter in the process. Frisken *et al.* [6] find that at low pressure, doubling the length of the channels does not significantly influence the final sizes of the produced vesicles. Our model corroborates experimental evidence at lower pressures but predicts that there is a length dependence at high pressure, which suggests further experimental investigation. Our model can also explain the small dependence in lipid concentration observed [6].

In addition to the rheological model, we performed out of equilibrium coarse-grained molecular dynamics simulations of vesicle extrusion to confirm our geometrical argument, to corroborate some main elements of Bruinsma's theory [10], and to describe the initial entry of a large vesicle in a nanochannel and its subsequent rupture. Although the extrusion of vesicles [11] and erythrocytes [12] has been simulated in the past, to the best of our knowledge, no true bilayer vesicle in an explicit solvent has ever been simulated in such a context. We leverage the computing power of graphical processing units (GPUs) to make this feasible in a relatively short time frame.

Our model and study should be useful to experimentalists considering pressure extrusion as a means to produce liposomes, but also to the large community studying the flow of diverse cells in and out of narrow channels such as red blood and plasma cells flowing in narrow capillaries.

II. EXTRUSION MODEL

The production of liposomes or SUVs through pressure extrusion consists in starting with a suspension of large and possibly multilamellar vesicles (MLVs) that is pushed by a pressure drop ΔP multiple times through an array of nanochannels of average radius R_p and length L_p as seen in Fig. 1 (typically 10–15 times [5–7]). For every passage through the extruder there is an ever-diminishing drop in the average vesicle size (see Fig. 1 in the article by Frisken *et al.* [6]).

*bjooos@uottawa.ca

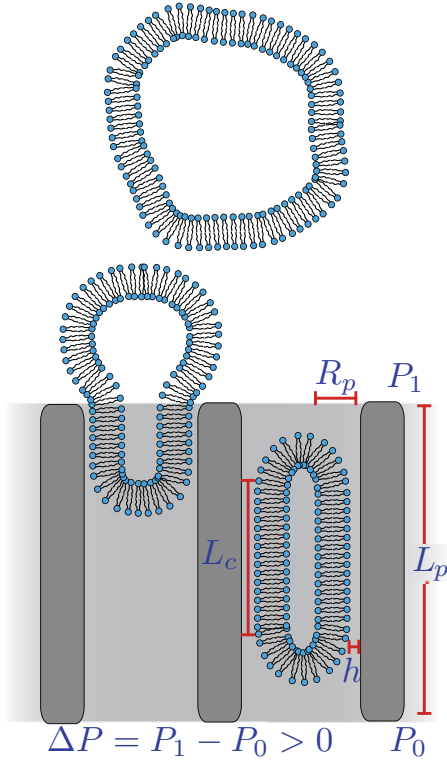


FIG. 1. (Color online) In the final passages, vesicles flow through the extruder back and forth going from a roughly spherical shape outside to a spherocylindrical shape inside. Some key variables are highlighted.

Toward the end of the entire extrusion procedure, most vesicles in suspension are unilamellar [7] and flow in and out of the nanochannels without rupturing. To a first approximation, we assume that in these last passages they transition from a nearly spherical shape outside the nanochannels to a spherocylindrical shape inside and back again while conserving volume as depicted in Fig. 1. Let us develop this argument.

A. Surface and volume conservation

We start with a vesicle of apparent initial spherical area $A_0 = 4\pi R_0^2$ enclosing a volume $V_0 = 4\pi R_0^3/3$. The membrane tension γ is related to its fractional surface expansion $\alpha = \Delta A/A_0$ by:

$$\alpha = \frac{k_b T}{8\pi k_c} \ln \left(1 + c \frac{\gamma A}{k_c} \right) + \frac{\gamma}{K_A}, \quad (1)$$

where K_A is the area compression modulus, k_c , the bending rigidity, and $c \simeq 0.1$ is a constant related to surface undulations [13]. For high enough tension, $\gamma \cong K_A \alpha$. Let us assume that in the extrusion process the vesicle volume stays constant while its area expands. Then there exists a critical value α_c where the vesicle ruptures. This critical surface expansion α_c can have two contributions: (1) α_A related to the flattening of the excess area in the membrane; (2) α_γ related to the lysis tension in the bilayer which depends on the nature of the lipids [see Eq. (1)]. Thus, $\alpha_c = \alpha_A + \alpha_\gamma$.

If the vesicle is pushed almost quasistatically in a nanochannel of radius R_p , it will do so without breaking as long as the

surface expansion remains below a threshold characterized by α_c . Assuming the steady-state shape in the channel to be that of a spherocylinder of side length L_c and radius R_p (see Fig. 1 with $h = 0$), we can find the critical vesicle to channel radius ratio $R = R_0/R_p$ for which the vesicle barely remains intact by solving the following derived polynomial:

$$V_0 = \frac{4\pi R_0^3}{3} = \pi L_c R_p^2 + \frac{4\pi R_p^3}{3} = V_f, \quad (2)$$

$$(1 + \alpha_c)A_0 = (1 + \alpha_c)4\pi R_0^2 = 2\pi L_c R_p + 4\pi R_p^2 = A_f, \quad (3)$$

$$2R^3 - 3(1 + \alpha_c)R^2 + 1 = 0. \quad (4)$$

Equation (2) accounts for volume conservation and Eq. (3) accounts for surface expansion, here assumed equal over the entire deformed vesicle. Combining Eqs. (2) and (3) leads to Eq. (4). It will be shown in Sec. III that Eq. (4) alone gives a rough approximation of the final size vesicles obtained by pressure extrusion. The next subsection extends our model to account for the pressure dependence.

B. Pressure dependence

Between the surface of a spherocylindrical vesicle and the surface of the channel it is flowing through, there is a relatively thin lubrication layer of thickness h (see Fig. 1 and inset of Fig. 5 for a close-up in simulations) that grows with increasing vesicle velocity U . The vesicle essentially travels in a channel of effective radius $R_{\text{eff}} = R_p - h$ that decreases with U and solving Eq. (4) in this case gives the ratio $R' = R_0/R_{\text{eff}}$. Thus, if we wish to get the corrected ratio $R = R_0/R_p$ for a given applied pressure ΔP we first need to calculate h . Bruinsma has given an expression for h as a function of U [10]:

$$h \cong 2.05 R_p \left(\frac{\eta U}{\gamma_f} \right)^{2/3}, \quad (5)$$

where η is the solvent's viscosity and γ_f is the frontal membrane tension of the vesicle. The membrane tension γ is predicted to be linearly decreasing along the cylindrical part of the traveling spherocylindrical vesicle going from γ_f at the front cap ($z = 0$) to γ_r at the rear cap ($z = L_c$), such that

$$\gamma(z) = \gamma_f - \frac{\eta U}{h(U)} z. \quad (6)$$

However, we will assume a uniform mean tension $\bar{\gamma}$ along the length of vesicle to simplify our calculations such that $\gamma_f \cong \bar{\gamma}$ in Eq. (5). Bruinsma also developed a Darcy-type law to describe the flow of spherocylindrical vesicles in narrow channels. First, he assumed that each of the N vesicles in a channel of length L_p at a given time diminishes the pressure drop ΔP across the whole channel by an amount $\Delta P^*(U)$, such that Poiseuille's law becomes

$$\eta U = \frac{R^2}{8} \left(\frac{\Delta P}{L_p} - n \Delta P^*(U) \right), \quad (7)$$

where $n = N/L_p$ is the linear density of vesicles in the channel. He then equated the energy dissipated in the lubrication layer to the work done by the pressure differential to drive the system and obtained a Darcy-like equation with an effective

channel permeability K' , which depends on the velocity U :

$$\eta U = K' \frac{\Delta P}{L_p} = \frac{R_p^2/8}{1 + nR_p L_c/4h(U)} \frac{\Delta P}{L_p}. \quad (8)$$

Since the mean flow velocity inside a channel is roughly equal to U , the above can be converted to a flow rate $Q \cong \frac{\pi R_p^2 K'}{\eta} \frac{\Delta P}{L_p}$. Supposing the vesicles flowing back and forth in the extruder can only barely support it without rupturing, we can make $\bar{\gamma} = \gamma_l$, the lysis tension, and calculate the ratio $R = R_0/R_p$ at a given pressure ΔP iteratively until the solution converges using Eq. (8) for the velocity U :

- $R(R_p, \Delta P, \alpha_c) = \{$
- (1) Calculate R' by solving Eq. (4) for a given α_c
 - (2) Estimate L_c using Eq. (2)
 - (3) Estimate h using Eqs. (5) and (8)
 - (4) Calculate $R_{\text{eff}} = R_p - h$
 - (5) Improve L_c using $R_p = R_{\text{eff}}$ with R' in Eq. (3)
 - (6) Improve h using the new value of L_c
 - (7) Repeat steps 3 to 5 until h and L_c converge
 - (8) Get R from h and R'
- $\} \quad (9)$

This is our complete model to predict the final size of extruded vesicles. Let us now discuss its agreement with experimental results.

III. MODEL AGREEMENT WITH EXPERIMENT

Let us consider vesicles made of POPC lipids such as in Patty and Frisken's study [7] with $K_A \cong 234$ mN/m, $k_c \cong 1.43 \times 10^{-19}$ J, $\gamma_l \cong 7.4$ mN/m, $R_p = [25, 50]$ nm, and $L_p = 6$ μ m. Using Eq. (1) we find $\alpha_\gamma \cong 0.04$. Solving Eq. (4) with this value for α_c gives $R = 1.23$ regardless of channel radius or applied pressure. In Fig. 2 we reproduced data that originated from pressure extrusion experiments performed by Patty and Frisken on POPC lipid vesicles [7]. Our value of R predicts the smallest vesicle sizes obtained by extrusion under strong pressure gradients, whereas we would have expected a better prediction for the final sizes under the weakest pressures. With $\alpha_c \cong 0.10$ we achieve this. Consequently, the final vesicles must be deflated with an excess area accounting for roughly 6% of the observed expansion ($\alpha_A \cong 0.06$), which is confirmed by the swelling they undergo at the end of the extrusion runs [14]. Although quite simplistic, we are convinced that our geometrical argument shows that to predict the final sizes of extruded vesicles one needs to describe how these objects flow through nanochannels.

Let us now include the pressure dependence. We fitted Eq. (9) to data from Patty and Frisken's paper [7]. We let α_c be a free parameter and used all other parameters therein except n that we fix to a value of $1/L_p \cong 1.67 \times 10^{-7}$ m $^{-1}$, a single vesicle per channel, which would correspond to a low lipid concentration. The model only weakly depends on n . Figure 2 shows the best fits and Table I gives the values for α_c as a function of the channel radius. The fits are in good agreement with the data. All expansion coefficients compare favorably with one another and are close to the upper limit $\alpha_c = 0.10$ considered in the geometrical argument for vesicles slightly

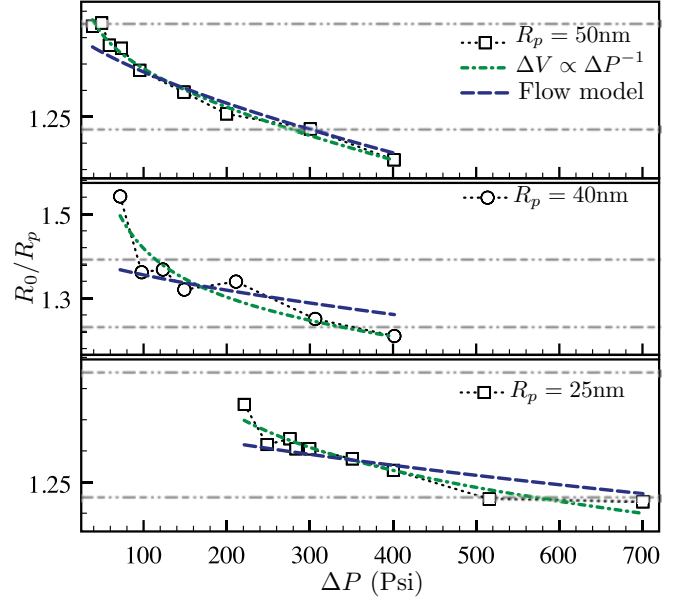


FIG. 2. (Color online) Experimental data of final vesicle sizes expressed in terms of the ratio $R = R_0/R_p$ as a function of the pressure drop ΔP for three different channel sizes are reproduced from Patty and Frisken's paper [7]. The horizontal gray dot-dashed lines are those for $\alpha_c = 0.04$ at $R = 1.23$ and $\alpha_c = 0.10$ at $R = 1.39$. The blue dashed lines represent the fits of our flow model, while the green dot-dashed lines are those with the volume relaxation argument included.

deflated with some excess area. Our model does not predict correctly the ratio R for the very lowest pressures especially for $R_p = 40$ nm. We think this is where one needs to pay careful attention to the first few passages in the extruder. It is quite possible that at lower pressures, the probability of forming large deflated vesicles with much excess area and reduced volume is greater. To account for this in our model we can potentially relax the volume by introducing a $\Delta V \propto \Delta P^{-1}$, which allows to better fit the data, but by doing so we need to introduce a free parameter hard to relate to the actual physics in the system. We show the resulting fits in Fig. 2 for the sake of completeness, although we will not further use this volume relaxation argument in the following discussion.

We took our flow model with the values of α_c we obtained and doubled the channel length L_p as in the paper by Frisken *et al.* [6], where they report no significant change in the final vesicle sizes at low pressure. Given the apparent experimental uncertainties, we show in Fig. 3 (top plot) that our model recovers that result since all curves seem to converge at low pressure. Indeed, in this limit where the flow rate is weakest, vesicle size is mostly defined by the geometrical constraints.

TABLE I. The mean critical surface expansion α_c obtained while fitting data from Patty and Frisken's paper [7] is roughly 0.10.

Channel radius R_p (nm)	Critical surface expansion α_c
25	0.083 ± 0.002
40	0.111 ± 0.005
50	0.105 ± 0.003

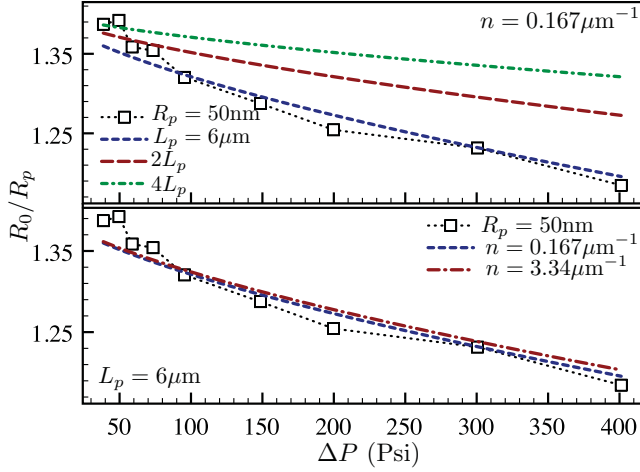


FIG. 3. (Color online) Top plot: compared to the reference (bottom blue line), doubling (middle red line), or even quadrupling (top green line) the channel length does not change much the final vesicle sizes at lower pressures, which corroborates previous findings [6]. The difference is much more important at higher pressures. Bottom plot: increasing the initial lipid concentration inevitably increases the number of vesicles in a given channel and reduces the flow rate, which results in slightly bigger final vesicles as previously observed [6].

However, we predict that at higher pressures the final mean vesicle size strongly depends on channel length or flow rate if one prefers as they are related. In fact, if the reduced vesicle size R is plotted as a function of the flow rate Q proportional to the pressure gradient $\Delta P/(\text{channellength})$, the theoretical predictions in Fig. 3 collapse onto a single curve (not shown). We therefore suggest revisiting the channel length doubling experiment at a higher pressure to test the validity of our prediction.

Interestingly, the flow rate dependence can also explain a result reported in the same paper [6], which is vesicle size weakly increases with lipid concentration. A higher lipid concentration results in an increase in n , the vesicle density in the channel, thus decreasing the flow rate Q . By increasing n twentyfold, roughly the limit density of vesicles in a channel before they start interacting, our model predicts a slight increase in the average vesicle size, which is coherent with experimental observations (see Fig. 3, bottom plot). However, the increase is more significant in Ref. [6]. This is most probably due to our approximation of a constant n for all pressure drops ΔP . Indeed, as ΔP increases, the size of vesicles traveling in the channel without rupturing decreases, which could lead to a slight increase in n .

IV. CGMD SIMULATIONS OF THE EXTRUSION PROCESS

Our flow model presented in Sec. II predicts the final sizes of extruded vesicles based on an analysis of the last few passages in a pressure extrusion run where size is expected to vary only marginally. It combines a geometrical argument (Sec. II A) to elements of Bruinsma's description of spherocylindrical vesicles flowing down narrow channels (Sec. II B). Using a coarse-grained molecular dynamics (CGMD) model, we thus decided to simulate small inflated and spherical lipid bilayer

vesicles being pressure extruded in channels of different sizes to corroborate qualitatively if not quantitatively the various components of our model (Sec. IV B). We also simulated larger vesicles extruded in the same narrow channels to give a qualitative description of the initial extrusion passages (Sec. IV C).

A. Simulation details

1. Model

We first performed CGMD simulations of planar lipid bilayer systems. We modeled all interactions using Goetz and Lipowsky's set of potentials [15] where σ is the unit of length, ϵ , of energy, τ , of time, and m , of mass. We chose a thermal energy $k_B T = 1.0\epsilon$ for all our simulations. We used lipids with one bead for the hydrophilic head and two beads for the hydrophobic tail. The lipids are fully flexible with no bending potential along their length. The hydrophilic solvent is of the Lennard-Jones (LJ) type with a density of $0.8\sigma^{-3}$ and shear viscosity $\eta = 1.98 \pm 0.16\sigma^{-2}\sqrt{m\epsilon}$ as calculated using Green-Kubo's formulation [16], in agreement with Ref. [17]. We characterized flat bilayers made of these short lipids and immersed in such a solvent. From the calculation of the microscopic stress tensor [15], we found $a_0 \cong 1.9\sigma^2$, the area per lipid at which the stress is zero with a bilayer thickness $l_{BM} \cong 4.8\sigma$, and an area compression modulus $K_A = 8.84 \pm 0.76\epsilon/\sigma^2$. We then calculated the bending rigidity using its relation to the area compression modulus [18] $k_c = K_A l_{BM}^2/48 = 4.24 \pm 0.36\epsilon$. As expected, our membranes are softer than those studied by Goetz and Lipowsky made of lipids with longer tails in a solvent of lower density at a slightly higher temperature [15,18].

2. Vesicles

We then prepared lipid bilayer vesicles made of our lipids suspended in the same LJ fluid using the ESPResSo package [19] with the included *mbtools* toolbox for lipid bilayer systems. Vesicles were all initially set up artificially such that the bilayer was under no stress due to a pressure difference between the inside and the outside [Fig. 4(a)]. No lipid flips were observed. Pressures were calculated using the diagonal components of the stress tensor. In this state, the lipid bead density across the membrane was found to be close to that of the fluid $\rho_{lip} = 0.8\sigma^{-3}$ with a profile in accordance with realistic simulations of vesicle self-assembly conducted by Marrink and Mark [20].

3. Extrusion through narrow channels

Finally, each vesicle was inserted in a large system made of two reservoirs linked by a channel of radius R_p and length L_p in a box periodic in all three directions. Each vesicle was pressure extruded through the narrow channel whose walls consisted in solvent beads laid out on an FCC lattice with density $1.0\sigma^{-3}$ and anchored in space with stiff harmonic springs [21]. We used the nonconservative part of dissipative particle dynamics (DPD) interactions to thermostat the system to a thermal energy $k_B T = 1.0\epsilon$ as they allow for momentum propagation [22], an essential feature to study flows (out of equilibrium dynamics). The anchored particles making up the wall interact with the rest of the system through DPD

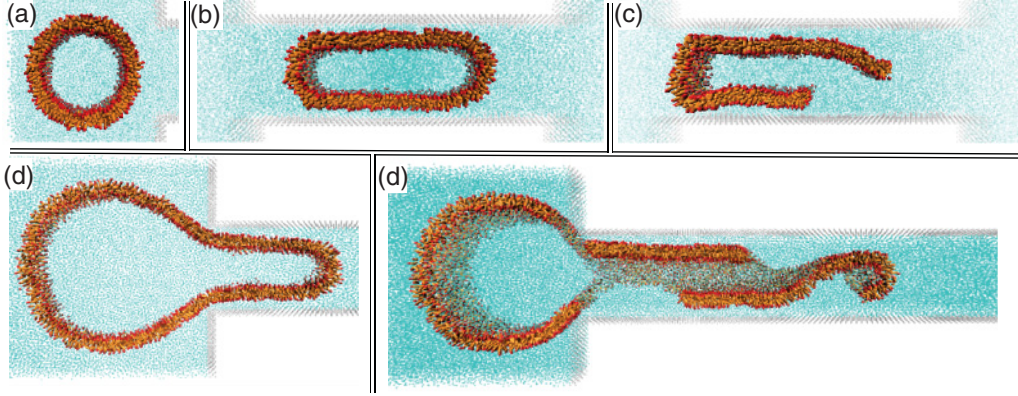


FIG. 4. (Color online) Slices from 3D simulations of the pressure extrusion of vesicles in nanochannels. (a) The initial shape of the vesicle for reference. (b) A spherocylindrical vesicle flowing in the channel. (c) A spherocylindrical vesicle breaking in a channel while pushed by a strong pressure difference. (d) The typical shape of a vesicle as it is entering the channel. (e) The rupture of a large vesicle at the entrance of a small channel.

interactions such that friction is reproduced in their vicinity. Indeed, simulations of the LJ fluid alone flowing under a pressure gradient yields a Poiseuille flow inside the channel with a negligible slip length, the velocity being essentially zero at the wall (data not shown). Pressure extrusion simulations were executed on graphical processing units (GPUs) using a customized version of the very fast and optimized HOOMD-Blue package [23,24] with an implementation of DPD [25]. Simulations ran on Sharcnet's Angel cluster, which contains 44 NVIDIA Tesla 1070 GPUs. Of course, even with a decent amount of computation power it always remained beyond our ability to simulate a suspension of multiple vesicles pressure extruded multiple times. But we can learn much from the study of the extrusion of a single vesicle.

4. Units

The SI units corresponding to the dimensionless quantities we use are not well defined as mentioned in Ref. [15]. Hence, the following only serves as a guide. We assume that our lipids are very crude approximations of two tails lipids: each tail bead is twice five CH_2 groups, which defines a length scale of $\sigma \cong 0.6$ nm and a mass scale $N_A m \cong 140$ g/mol according to Ref. [26]. The energy scale is fixed at $N_A \epsilon \cong N_A k_B 310$ K = 2.6 kJ/mol. This gives a time scale $\tau = 4.4$ ps such that the duration of extrusion events in our short channels is on the tens of nanosecond scale. Other typical values are: $\Delta P = [290, 2300]$ psi, $U \sim 2$ m/s, and $Q \sim 4 \times 10^{-10}$ ml/s ($R_p \cong 8$ nm and $L_p \cong 60$ nm). For comparison, in the studies conducted by Frisken *et al.* [5–7], $\Delta P = [0, 700]$ psi, $U \sim 0.3$ m/s, and $Q \sim 10^{-10} - 10^{-9}$ ml/s, which means we would be in the right range.

B. Final passages simulated

The extrusion in nanochannels of small vesicles made of $n_l = 3000$ lipids was simulated. Once setup and equilibrated, the vesicles were composed of an outer layer made of $n_{\text{out}} = 1841$ lipids with a mean area per lipid head $a_{\text{out}} = 1.86\sigma^2$, which corresponds to a radius of $R_{0,\text{out}} = 16.5\sigma$, while the corresponding values of the inner layer $n_{\text{in}} = 1159$, $a_{\text{in}} = 1.68\sigma^2$, and $R_{0,\text{in}} = 11.5\sigma$. The inner heads are more

compressed than the outer heads, which is characteristic of self-assembled SUVs [20]. Overall the area per lipid of our vesicles is smaller than $a_0 = 1.9\sigma^2$ found for flat bilayer membranes. This is mainly due to the difference in geometry and the finite size of our systems.

1. Geometrical argument

We tracked multiple observables throughout our simulations, one of the most important being the local area per lipid a , which is directly related to the stress in the bilayer. It was calculated from the triangulation of both the outer and inner layers using the Crust surface reconstruction algorithm [27] while accounting for lipid flips from one layer to the other. Following a and its mean \bar{a} permitted us to determine both the time and the spatial coordinates of a rupture event. The observation of many such events [Fig. 4(c)] leads to values of the expansion coefficient for both layers very close to one another: $\alpha_{c,\text{out}} \cong \alpha_{c,\text{in}} \equiv \alpha_c \cong 0.21$. Feeding this α_c into Eq. (4) gives a ratio $R = R_0/R_p = 1.62$. Taking $R_0 = R_{0,\text{in}}$, we find $R_{p,\text{crit}} = 10.2\sigma$, the smallest channel radius into which the vesicle can penetrate and travel without breaking. Now in our simulations, even at the lowest pressures, there is a lubrication layer between the vesicle and the channel wall of minimal thickness close to the size of a LJ bead $h_{\text{min}} \cong 1.1\sigma$. We thus need to compare the predicted critical radius with the minimal effective radius $R_{\text{eff}} = R_p - h_{\text{min}}$. Because our walls were set up on a lattice to maximize impermeability, we could not fine tune the radius to a very specific value, but when $R_p = 12.0\sigma$, that is $R_{\text{eff}} = 10.9\sigma$, we could barely push vesicles in without breaking them while for $R_p = 11.5\sigma$, $R_{\text{eff}} = 10.4\sigma$, it appeared impossible on the time scale of our simulations. Thus, the true size limit is most probably very close to the one predicted by the geometrical argument.

2. The lubrication layer

We measured the thickness of the lubrication layer h and can assert that it does increase with the mean flow velocity U as predicted by Bruinsma [10]. To our knowledge, this is the first direct measurement of h for a vesicle flowing in a narrow channel. We show in Fig. 5 the cumulative data for vesicles

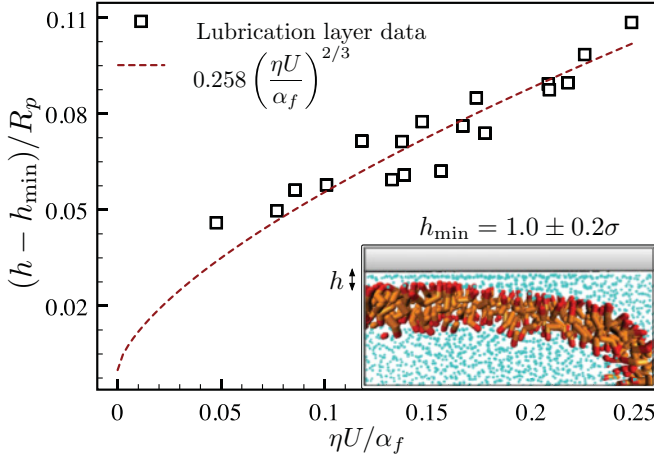


FIG. 5. (Color online) The lubrication layer's thickness h grows with $\eta U/\gamma_f$ as predicted by Bruinsma [10]. Here we used α_f , the frontal area per lipid expansion of the outer layer of the membrane of our spherocylindrical vesicles traveling in channels that we assume goes like γ_f , the frontal tension in the membrane.

flowing in channels of radii $R_p = \{13.0, 13.5, 14.0\}\sigma$ plotted using nondimensional axes $(h - h_{\min})/R_p$ versus $\eta U/\alpha_f(U)$, where α_f is the frontal area per lipid expansion of the vesicles, $\eta = 1.98\sigma^{-2}\sqrt{m\epsilon}$ is the shear viscosity of the surrounding LJ fluid, and $h_{\min} = 1.0 \pm 0.2$ is the minimum thickness of the lubrication layer whose value was extracted by fitting the data. One can see that the expected power law behavior with an exponent of $2/3$ agrees well with our data. Furthermore, the minimal thickness h_{\min} found corresponds to the approximate value we can directly extract from simulations at the lowest pressures (see Sec. IV B1). Fluid particles within a distance h_{\min} away from the channel wall move with a velocity roughly an order of magnitude slower than the vesicle and close to zero such that they essentially create a no-slip layer. This is in agreement with what we found for a simple LJ fluid flow.

3. Darcy's law

The actual relationship between flow velocity and pressure may be written as $\eta U = K'(\Delta P - \Delta P_{\min})/L_p$ [6] where ΔP_{\min} is the minimum pressure to push a vesicle of given size in the channel and K' is defined in Eq. (8). We plotted, in Fig. 6, ΔP as a function of UL_p/K' for data from simulations of small vesicles made of $n_l = 3000$ lipids pushed in channels of radii $R_p = \{13.0, 13.5, 14.0\}\sigma$ and extracted the shear viscosity η of the fluid in the lubrication layer and a mean minimum pressure ΔP_{\min} .

The table at the top of Fig. 6 summarizes the results. The shear viscosities reported in Fig. 6 are all within the margins of uncertainty of the expected value (see Sec. IV A 1), a remarkable result given the number of physical quantities entering the calculation. Any small change to these produces important deviations in the value of η . As for the minimal pressure, one would expect it to decrease as the radius of the channel increases, and this is what we observe: it is harder to push a vesicle of a given size in a smaller channel. However, we were not able to directly verify the accuracy of these predicted values in our simulations due to time constraints (very long and multiple massive simulations necessary).

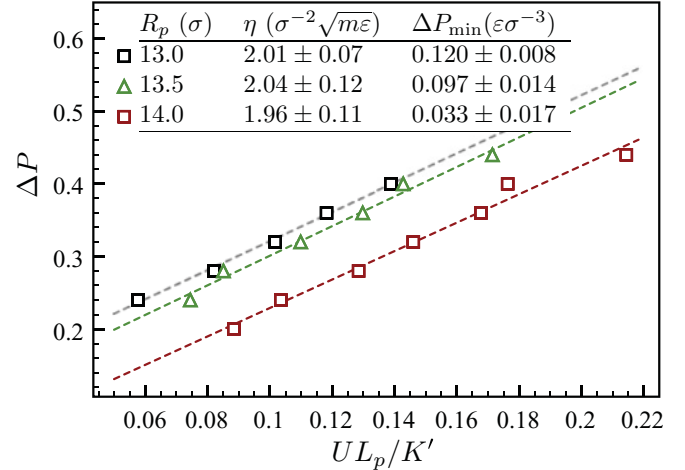


FIG. 6. (Color online) Verifying that Darcy's law of the form $\eta U = K'(\Delta P - \Delta P_{\min})/L_p$ holds for our simulated vesicles. We here show linear plots of ΔP as a function of UL_p/K' for various channel radii $R_p = \{13.0, 13.5, 14.0\}\sigma$. The slope is the shear viscosity η and the intercept, the minimum pressure ΔP_{\min} .

4. Tension profile along the vesicle

Figure 7(b) gives a visual representation of the shape and tension map of a spherocylindrical vesicle traveling down a narrow channel. The tension corresponds to the mean area expansion averaged over the two leaflets. A quick look clearly shows that the most probable location for pore nucleation is just behind the frontal cap where the cylindrical part starts. Our observation of multiple rupture events inside the channel at high pressures confirm this. In the cylindrical portion, the tension is observed to decrease from front to back as predicted by Bruinsma [10]. To directly test the relationship between tension γ and distance z along the vesicle expressed in Eq. (6), we plotted the area expansion factor profiles $\alpha(z)$

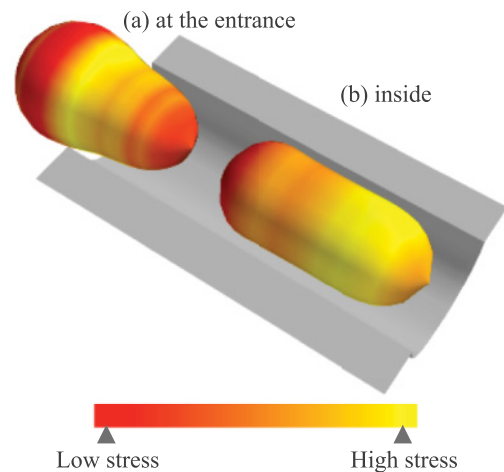


FIG. 7. (Color online) Vesicle shapes and colors mapped according to the total tension in the bilayer calculated from the mean area expansion as it enters the nanochannel (a) and as it travels inside in a spherocylindrical shape (b). When at the entrance, the stress is greatest in the neck region where pore nucleation and subsequent rupture is most probable, while it appears this maximum is just behind the frontal part when inside.

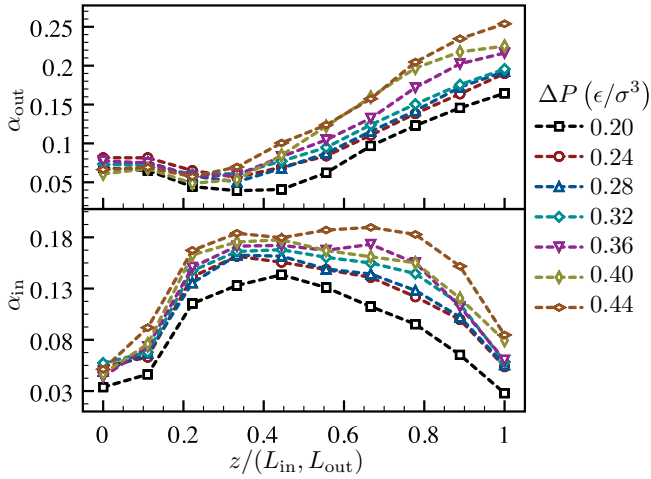


FIG. 8. (Color online) Average tension profiles for the outer and inner layers of the membrane inferred from the change in area per lipid α as the spherocylindrical vesicles travel down the channel. The z coordinate along the length of the objects has been renormalized for ease of calculation and clarity. One can clearly observe, in the outer layer, the linear decrease of tension going from the frontal cap of the vesicle to its back.

as measured at both the inner and outer head groups in Fig. 8. Assuming we are in a linear regime where $\gamma \cong K_A \alpha$ we find that the profile for the outer layer of the membrane $\alpha_{\text{out}}(z)$ corroborates Eq. (6), that is the tension decreases linearly along the cylindrical part of the vesicle in the channel going from the front to the back. The slope of the linear part should be, according to the same equation, $\sim \eta U / K_A (h - h_{\text{min}})$. We thus extracted from our data an approximate value for the area compressibility modulus $K_A = 6.95 \pm 0.29 \epsilon / \sigma^2$. Although this value is not exactly equal to $K_A = 8.84 \pm 0.76 \epsilon / \sigma^2$ found for a flat bilayer (Sec. IV), it is of the same order of magnitude and still quite close. Our use of α_{out} in Eq. (6) is justified by the finite thickness of our membrane and the direct contact between the outer heads and the lubrication layer. If Bruinsma considered the full tension in the membrane, he did so while assuming a negligible thickness which we cannot.

Interestingly, the area expansion profile for the inner layer $\alpha_{\text{in}}(z)$ of the membrane does not follow its outer counterpart $\alpha_{\text{out}}(z)$. Indeed, α_{in} is roughly constant along the cylindrical part of the vesicle which means the hydrodynamic shear stresses the outer membrane is subjected to get damped in the bilayer and do not propagate to the inner heads. At the back of the vesicle, the hydrodynamic stress on the outer layer is at its lowest and the stresses on the two layers are comparable. As for the frontal part, the high curvature spaces out the outer heads while it compresses the inner heads, which enhances the difference in area expansion between the two leaflets. This effect will diminish with increasing vesicle size. It is not clear whether it will impact the expected location of the rupture point.

C. Initial passages simulated

To produce small vesicles by pressure extrusion, one starts with a suspension of rather large vesicles that break into smaller and smaller pieces with each passage through the extruder until the size stabilizes. Until now one could only

guess the true mechanics of rupture of these large initial vesicles. For instance, it has been proposed that rupture occurs at the neck of the channel in an axisymmetric fashion such that small hemispherical vesicles are expressed from the larger ones (“blowing a bubble” model of Patty and Frisken [7]). We show that, in the initial passages, the neck is indeed the most probable location for a rupture event via pore nucleation [see Fig. 7(a)] but that it often occurs in multiple sites at the same time [see Fig. 4(e)].

In our simulations, a rather large vesicle ($n_l = 10,000$) approaching a small channel ($R_p = 12.0\sigma$) in a converging flow field eventually gets sucked-in due to the hydrodynamic friction with fluid particles speeding by as they enter the channel. Figure 4(d) shows the vesicle as it is squeezing in the channel. Then one of two scenarios can happen: (1) the pressure is too weak and the vesicle reaches an equilibrium state; (2) the pressure is strong enough leading to rupture. When the vesicle ruptures, it always does so through pore nucleation whose probability is greater in the neck region, as shown in Fig. 7(a). However, the cylindrical portion of the vesicle in the channel is also under considerable stress. Thus, pores often nucleate in multiple sites at the same time, which gives rise to flowing lipid sheets along the channel as shown in Fig. 4(e). The sheets can then rip apart into smaller pieces in the channel and drift toward the other end where they fold again into floppy, partly deflated smaller vesicles. We think that the slightly higher than expected values of the critical surface expansion coefficient α_c that we found while analyzing results from Patty and Frisken [7] are in part due to that loss of total internal volume or, equivalently, the creation of excess area. The polydispersity observed in the final sizes of vesicles produced by pressure extrusion [5–7] is most probably a direct consequence of the stochastic nature of the rupture of large vesicles penetrating into channels of small opening.

V. CONCLUSION

In the first part of this article, we have shown that the mean final size of vesicles produced by pressure extrusion depends on two elements: the geometrical constraints imposed on the vesicles due to volume conservation and finite extensibility, and the flow rate. It is known that beyond a critical area expansion α_c , a lipid bilayer vesicle ruptures and that the transition from a spherical shape outside the channel to a spherocylindrical shape inside is one that inevitably stretches its membrane if volume is to be conserved: a narrower channel results in greater area expansion. In addition, the faster a spherocylindrical vesicle travels inside the channel the more its membrane stretches since the channel appears smaller as a result of the thickening of the lubrication layer surrounding it [10]. Hence, as the flow rate increases, the size of vesicles that can go through a given channel without breaking decreases. Our model captures this behavior and predicts the mean final size of vesicles obtained by pressure extrusion given the lysis tension γ_l and related approximate critical area expansion α_c of a lipid bilayer, the radius R_p and length L_p of the extruder’s channels, and the applied pressure ΔP . Flow rate can be varied in multiple ways, the easiest being a change in either the pressure gradient $\Delta P / L_p$ or the channel radius R_p . More subtly, Eq. (8) shows that an increase

in lipid concentration results in a greater density of vesicles per channel, which decreases the flow rate and produces slightly larger final vesicles. To test our model and in particular the flow rate dependence, we propose that the simple channel length doubling experiment performed at low pressure in the paper by Frisken *et al.* [6], where they observed no significant difference in the mean final size of extruded vesicles, should be repeated at high pressure, where we predict a large vesicle size difference.

Fitting experimental data yields an effective critical expansion parameter α_c of the bilayer, which includes both the unfolding component α_A and the expansion component α_γ . α_γ is usually known, so the fitting will yield α_A a measure of the degree of floppiness of the vesicle. α_A can then be used to estimate the content loss through the entire extrusion process, as volume loss is an important generator of excess area. This could potentially be useful in the context of drug encapsulation prior to extrusion.

In our model, we assumed a uniform tension along the length of the spherocylindrical vesicle to be able to derive a set of equations that we could numerically solve. Although to us it appears like the appropriate thing to do given the context, we know it is not true from both the theory and our simulations. It would be interesting to see if a model that can account for a linear tension gradient can be constructed.

The second part of our paper presents results from large scale nonequilibrium coarse-grained molecular dynamics simulations of nanosized vesicles being extruded in narrow channels. Both lipids and solvent were explicitly included in the simulations, which to our knowledge is a first. Simulation costs in time and/or computing facilities has always been a major deterrent for doing so, but with the introduction of GPU-optimized code, it is now feasible on a reasonable time

scale with moderate resources. Ideally, a suspension of vesicles extruded multiple times through an array of channels would have been simulated to directly compare with our model. But this was too expensive in time and resources. Thus, only single vesicles being extruded were simulated to corroborate the elements of the model developed in the first part. The results of our simulations agree exceptionally well with Bruinsma's [10] description of a spherocylindrical vesicle flowing in a narrow channel and our own geometrical argument. We also used our simulations to try and give a qualitative description of the initial passages of large vesicles in the extruder. We showed that large vesicles did not rupture cleanly at the entrance of the channel but heterogeneously along the cylindrical part of the vesicle that is within the channel and with a greater probability in the neck region. The fragments would then flow down the channel to close again into smaller and floppier vesicles.

Rupture in the channel of small extruded vesicles was frequently observed near the critical size. It always occurs close to the front cap, which a careful analysis of the tension profile can explain, and it is always accompanied by content loss and eventual closure of nucleated pores. A detailed study of this phenomenon will be presented in a subsequent paper. It should appeal to those interested in the encapsulation and release of drugs in the body and to those studying the flow-induced rupture of red blood cells in small capillaries, since vesicles have similar rheological properties.

ACKNOWLEDGMENTS

The work has been funded in part by the Natural Sciences and Engineering Research Council (Canada). The authors thank C. E. Morris for a critical reading of the manuscript.

-
- [1] A. Jesorka and O. Orwar, *Annu. Rev. Anal. Chem.* **1**, 801 (2008).
 - [2] D. Fenske, A. Chonn, and P. Cullis, *Toxicol. Pathol.* **36**, 21 (2008).
 - [3] B. Maherani, E. Arab-Tehrany, R. Mozafari, C. Gaiani, and M. Linder, *Current Nanoscience* **7**, 436 (2011).
 - [4] M. Hope, M. Bally, G. Webb, and P. Cullis, *Biochim. Biophys. Acta* **812**, 55 (1985).
 - [5] D. Hunter and B. Frisken, *Biophys. J.* **74**, 2996 (1998).
 - [6] B. Frisken, C. Asman, and P. Patty, *Langmuir* **16**, 928 (2000).
 - [7] P. Patty and B. Frisken, *Biophys. J.* **85**, 996 (2003).
 - [8] S. Clerc and T. Thompson, *Biophys. J.* **67**, 475 (1994).
 - [9] L. Rayleigh, *Proceedings of the London Mathematical Society* **1**, 4 (1878).
 - [10] R. Bruinsma, *Physica A: Stat. Theor. Phys.* **234**, 249 (1996).
 - [11] G. Gompper and D. M. Kroll, *Phys. Rev. E* **52**, 4198 (1995).
 - [12] D. Quinn, I. Pivkin, S. Wong, K. Chiam, M. Dao, G. Karniadakis, and S. Suresh, *Ann. Biomed. Eng.* **1** (2011).
 - [13] W. Rawicz, K. Olbrich, T. McIntosh, D. Needham, and E. Evans, *Biophys. J.* **79**, 328 (2000).
 - [14] B. Mui, P. Cullis, E. Evans, and T. Madden, *Biophys. J.* **64**, 443 (1993).
 - [15] R. Goetz and R. Lipowsky, *J. Chem. Phys.* **108**, 7397 (1998).
 - [16] M. Kenward and G. Slater, *Eur. Phys. J. E* **14**, 55 (2004).
 - [17] K. Meier, A. Laesecke, and S. Kabelac, *J. Chem. Phys.* **121**, 3671 (2004).
 - [18] R. Goetz, G. Gompper, and R. Lipowsky, *Phys. Rev. Lett.* **82**, 221 (1999).
 - [19] H. Limbach, A. Arnold, B. Mann, and C. Holm, *Comput. Phys. Commun.* **174**, 704 (2006).
 - [20] S. Marrink and A. Mark, *J. Am. Chem. Soc.* **125**, 15233 (2003).
 - [21] F. Tessier and G. Slater, *Macromolecules* **38**, 6752 (2005).
 - [22] T. Soddemann, B. Dünweg, and K. Kremer, *Phys. Rev. E* **68**, 046702 (2003).
 - [23] J. Anderson, C. Lorenz, and A. Travesset, *J. Comput. Phys.* **227**, 5342 (2008).
 - [24] A. Anderson and A. Travesset, *Comput. Sci. Eng.* **10** (2008).
 - [25] C. Phillips, J. Anderson, and S. Glotzer, *J. Comput. Phys.* **230**, 7191 (2011).
 - [26] E. Egberts and H. J. C. Berendsen, *J. Chem. Phys.* **89**, 3718 (1988).
 - [27] N. Amenta, M. Bern, and M. Kamvysselis, *Proceedings of the 25th Annual Conference on Computer Graphics and Interactive Techniques*, 415 (1998).